Sinopfbd, 2024; 9(1): 72-95 **https://doi.org/10.33484/sinopfbd.1370598**

Sinop Üniversitesi Fen Bilimleri Dergisi
Sinop Uni J Nat Sci
E-ISSN: 2564-7873

https://dergipark.org.tr/tr/pub/sinopfbd

Crystal Structure and Hirshfeld Surface Analysis of a Heterometallic Hofmann-Type-Like Compound

Zeki KARTAL[1] and Zarife Sibel ŞAHİN[2]

How to cite: Kartal, Z., & Şahin, Z. S. (2024). Crystal structure and Hirshfeld surface analysis of a heterometallic Hofmann-type-like compound. *Sinop Üniversitesi Fen Bilimleri Dergisi, 9*(1), 72-95. https://doi.org/10.33484/sinopfbd.1370598

Research Article

Corresponding Author
Zarife Sibel ŞAHİN
zarifesibel@sinop.edu.tr

ORCID of the Authors
Z.K: 0000-0001-9739-0858
Z.S.Ş: 0000-0003-2745-7871

Received: 04.10.2023
Accepted: 22.02.2024

Abstract

In this study; a new heterometallic compound defined by the open formula $[Cd(H_2O)_2Ni(CN)_4]_4[Cd(H_2O)_4Ni(CN)_4]_5$ was synthesized in crystal form. Consisting of components such as water molecules, $[Ni(CN)_4]^{2-}$ anions, and cadmium transition metal atoms, this new crystal structure has no analogues which might have been previously obtained, even with other transition metal atoms. It is a new compound and a unique example of a crystal. The structural properties of this heterometallic compound have been characterized by single crystal X-ray diffraction spectroscopy (SC-XRD), FT-IR spectroscopy, thermal analysis and elemental analysis methods. According to the data obtained from the SC-XRD technique, this heterometallic compound has a monoclinic crystal system and a *C2/c* space group. The asymmetric unit of this compound consists of five Cd(II) ions, five Ni(II) ions, eighteen cyanide ligands, and fourteen coordinated water ligand molecules. In addition, theoretical calculations have been made with the Gaussian 03 program in order to obtain more information about this heterometallic Hofmann-type-like compound. The chemical properties of this new compound have been calculated using its HOMO and LUMO values and the natural bond orbital (NBO) analyses. In addition, Hirshfeld surface analysis of the asymmetric unit of this compound has been performed with the CrystalExplorer program. As a result of the Hirshfeld surface analysis, extensive information has been obtained about the weak intramolecular and intermolecular forces that form this new crystalline compound.

Keywords: Hofmann-type-like compound, SC-XRD analysis, FT-IR spectroscopy, Theoretical calculations, Hirshfeld surface analysis

Heterometalik Hofmann Tipi Benzeri Bir Bileşiğin Kristal Yapısı ve Hirshfeld Yüzey Analizi

[1]Retired Professor, Kütahya, 43000, Türkiye

[2]Sinop University, Faculty of Engineering and Architecture, Department of Energy Systems Engineering, Sinop, 57000, Türkiye

Öz

Bu çalışmada; açık formül $[Cd(H_2O)_2Ni(CN)_4]_4[Cd(H_2O)_4Ni(CN)_4]_5$ ile tanımlanan yeni bir heterometalik bileşik, kristal formda sentezlendi. Su molekülleri, $[Ni(CN)_4]^{2-}$ anyonları ve kadmiyum geçiş metali atomları gibi bileşenlerden oluşan bu yeni kristal yapının, diğer geçiş metali atomlarıyla bile daha önce elde edilmiş olabilecek hiçbir analogu yoktur. Yeni bir bileşik ve kristalin eşsiz bir örneğidir. Bu heterometalik bileşiğin yapısal özellikleri, tek kristal X-ışını kırınım spektroskopisi (SC-XRD), FT-IR spektroskopisi, termal analiz ve elementel analiz yöntemleriyle karakterize edilmiştir. SC-XRD tekniğinden elde edilen

verilere göre bu heterometalik bileşik, monoklinik kristal sistemine ve *C2/c* uzay grubuna sahiptir. Bu bileşiğin asimetrik birimi beş Cd(II) iyonu, beş Ni(II) iyonu, on sekiz siyanür ligandı ve on dört koordineli su ligandı molekülünden oluşur. Ayrıca bu heterometalik Hofmann tipi bileşik hakkında daha fazla bilgi edinmek amacıyla Gaussian 03 programı ile teorik hesaplamalar yapılmıştır. Bu yeni bileşiğin kimyasal özellikleri, HOMO ve LUMO değerleri ve doğal bağ yörünge (NBO) analizleri kullanılarak hesaplandı. Ayrıca bu bileşiğin asimetrik biriminin Hirshfeld yüzey analizi CrystalExplorer programı ile yapılmıştır. Hirshfeld yüzey analizi sonucunda bu yeni kristal bileşiği oluşturan zayıf molekül içi ve moleküller arası kuvvetler hakkında kapsamlı bilgiler elde edildi.

Anahtar Kelimeler: Hofmann tipi bileşik, Tek-kristal XRD analizi, FT-IR spektroskopisi, Teorik hesaplamalar, Hirshfeld yüzey analizi

Introduction

In organic and inorganic chemistry, compounds obtained by reacting some metal atoms, especially transition metal atoms with some ligand molecules ionic groups, are called "coordination compounds" [1]. The coordination compounds are very interesting compounds in terms of their physical and chemical properties. The interest in them in the field of science is increasing along with the number of researchers working on coordination compounds and consequently the scientific research results published about them. As a result of the chemical interactions of carbon and nitrogen atoms, either uncharged groups or charged ionic groups can be formed, depending on the number of atoms involved and the type of bonds formed between them. One of these ionic groups is the cyanide group $(C\equiv N)^-$, which has a negative charge. In the formation of Hofmann-type and Hofmann-type-like compounds, compounds are obtained, $K_2Ni\ (CN)_4$ compound, which is formed chemically by the cyanide group with potassium atom and nickel atom, is the most widely used basis compound. [2]. By using the $K_2Ni\ (CN)_4$ compound, various ligand molecules and transition metal atoms, many different compounds from 1D to 3D can be obtained in powder form or crystal form. The general formulae of Hofmann type compounds and Hofmann-type-like compounds are given as $M(II)LNi(CN)_4$ and $M(II)LL'Ni(CN)_4$, respectively. In these formulae, the symbols L and L′ indicate different ligand molecules in the compounds. In Hofmann type compounds, the number of this ligand molecule can be 1 or at most 2 depending on the nature of the L ligand molecule [3-5]. Moreover, by replacing the Ni atom in the $Ni\ (CN)_4$ ion group with palladium (Pd) and platinum (Pt) atoms, new types of Hofmann compounds were formed, and by replacing Ni atom with zinc (Zn), cadmium (Cd) and mercury (Hg) atoms, Hofmann-T_d-type compounds were formed [3-5]. In Hofmann-type-like compounds, the number of these ligand molecules can be 1, 2, or more, depending on the nature of the L and L′ ligand molecules. In Hofmann-type-like compounds, the number of a single ligand molecule must be either one or more than two (never n equals two). The compounds formed in all these cases are the Hofmann-type-like compounds. Extensive information can be found on Hofmann-type compounds and Hofmann-type-like compounds in previous works by us and other researchers [6-19]. The results of adding another ligand molecule to the structure of Hofmann-type and Hofmann-type-like compounds formed by a kind of ligand with a transition metal atom can be examined by comparing their

spectroscopic and crystalline data. If the effect of the additional ligand or ligands increases the stability of the formed crystal structure, the storage volume and some other properties, this is a positive situation for newly obtained compounds. In a previous study, some new Hofmann-type compounds and Hofmann-type-like clathrates were obtained in powder and crystal form by using water molecules (H_2O), $K_2Ni(CN)_4$ compound and zinc (Zn) transition metal atoms [16, 18, 19]. The aim of this study is to synthesize Hofmann-type and Hofmann-type-like compounds in crystal form by using potassium tetracyanonickelate (II) monohydrate [$K_2Ni(CN)_4 \cdot H_2O$] compound, cadmium (II) chloride monohydrate ($CdCl_2 \cdot H_2O$) compound and water (H_2O) molecules. In these chemical processes, the water molecule acts as both a solvent and a ligand molecule. As a result of this study, it is expected to obtain a Hofmann-type compound or a Hofmann type water clathrate in crystal form. The chemical formula of this compound is either [$Cd(H_2O)_mNi(CN)_4$] ($m > 2$) or [$Cd(H_2O)_2Ni(CN)_4] \cdot n(H_2O)$ ($n = 1, 2, 3, \dots$) is expected. The "m" and "n" coefficients in the formulae show the number of ligand molecules in the compound and the number of guest molecules in the clathrate, respectively. No data matching or similar to all data were found for this Hofmann-type-like compound obtained in crystalline form. Therefore, this compound is currently a first in its field.

Experimental

Materials

In this study, all chemical compounds such as potassium tetracyanonickelate(II) monohydrate $K_2[Ni(CN)_4] \cdot H_2O$, (Fluka, 96%), cadmium(II) chloride monohydrate ($CdCl_2 \cdot H_2O$), (Sigma Aldrich, 99+ %), and ammonia solution (NH_3, Merck, 25%) were used to obtain the targeted compound.

Synthesis of Compounds with Formulae [$Cd(H_2O)_MNi(CN)_4$] or [$Cd(H_2O)_2Ni(CN)_4$]•$N(H_2O)$

The compound in question was obtained as a result of the following processes. 1 mmol of $K_2[Ni(CN)_4] \cdot H_2O$ (0.259 g) was dissolved in 10 mL of twice distilled hot water. The compound $CdCl_2 \cdot H_2O$ (0.202 g) was added to this solution. In this study, the distilled water was used both as a solvent and a ligand molecule. As a result of all these chemical reactions, Hofmann-type-like compound or Hofmann type water clathrate, whose open formula is thought to be [$Cd(H_2O)_mNi(CN)_4$] ($m > 2$) or [$Cd(H_2O)_2Ni(CN)_4] \cdot n(H_2O)$ ($n = 1, 2, 3, \dots$), was formed. It was a colorless suspension. By adding diluted ammonia solution to this medium, the medium was made more transparent and purified from all impurities in the medium. This clear mixture was stirred at 65°C for two hours, then filtered through the most tightly meshed filter paper and allowed to crystallize at room temperature. As a result of this study, after about two and a half months, a transparent, thin and long rod-like compound in crystalline form was obtained. The compounds formed by transition metal atoms in a chemical interaction environment with cyanide compounds, even with other ligand molecules and solvent molecules in the environment,

can occur in very different numbers and in structural conditions, depending on the number of cyanide ligands that bond [20, 21]. According to the data obtained from various techniques for this compound obtained in crystal form, it was understood that it is an example of a Hofmann-type-like compound. The full formula of this compound was determined as $[Cd\ (H_2O)_2Ni\ (CN)_4]_4[Cd(H_2O)_4Ni(CN)_4]_5$ as a result of various experimental studies. This compound will be denoted as **1** for short hereafter. The new crystalline compound obtained is a very specific example of Hofmann-type-like compounds, as it contains both a Hofmann-type compound with the formula $ML_2Ni\ (CN)_4$ and a Hofmann-type-like compound with the formula $ML_4Ni(CN)_4$ (see Figure 1).

Instrumentation

A suitable crystal of **1** was selected for data collection which was performed on a D8-QUEST diffractometer equipped with a graphite-monochromatic Mo-K_α radiation at 296 K. The structure was solved by direct methods using SHELXS-2013 [22] and refined by full-matrix least-squares methods on F^2 using SHELXL-2013 [23]. The H atoms were located in a difference map refined freely. The high residual electron densities (maxima and minima) and metal center separations are 0.964 and 0.849 Å. Therefore, these high residual electron densities could not be defined from the refinement of the structure. The following procedures were implemented in our analysis: data collection: Bruker APEX2 [24]; program used for molecular graphics were as follows: MERCURY programs [25]; software used to prepare material for publication: WinGX [26]. The FT-IR spectrum of compound **1** was gained immediately as soon as the crystal was obtained under normal laboratory conditions using the Bruker Optics Vertex 70 FT-IR Spectrometer (3650 – 400) cm^{-1} wavenumber range, 2 cm^{-1} resolution, using the KBr technique. The metal amounts in the structure of compound **1** were analyzed with the Perkin-Elmer optima 4300 DV ICP-OES device, and the carbon, nitrogen and hydrogen amounts were analyzed with the CHNS-932 (LECO) elemental measuring device. TG and DTG analysis curves of the thermal behavior of compound **1** were recorded with an SII EXSTAR 6000 TG/DTA 6300 thermal analyzer in a temperature range (20–800) °C at a heating rate of 5 °C/min in the nitrogen atmosphere. Since there is an FT-IR device in our laboratory, FT-IR spectra of all compounds in powder or crystal form can be obtained by us as soon as possible. However, since the analysis of the elements in the structure of any compound or the SC-XRD structure analysis is carried out with devices in other departments or even in other cities of our institution, these processes can take place after a very long time after the synthesis of the compound. Some changes in the structure of some compounds (such as loss of water and guest molecules) may occur during this long period of time. For this reason, some differences may occur between the FT-IR results of some compounds and the elemental analysis and SC-XRD results. A similar situation for compound **1** is described in section 3.3.1.

Results and Discussion

Crystallographic Analysis of Compound 1.

The experimentally measured and theoretically calculated amounts of C, H, N, Cd and Ni atoms in the structure of compound **1** are listed in Table 1.

Table 1 *Elemental analysis of compound* ***1***.

Open formula of compound 1 and its molecular mass M_r (g)	Elemental analysis, found (%) / (calculated) (%)				
	C	**H**	**N**	**Cd**	**Ni**
$[Cd(H_2O)_2Ni(CN)_4]_4[Cd(H_2O)_4Ni(CN)_4]_5$	14.19	1.95	17.06	34.03	17.35
M_r = 2980.99	(14.50)	(1.89)	(16.93)	(33.94)	(17.72)

The asymmetric unit of the heterometallic compound **1** consists of five Cd (II) ions, five Ni (II) ions, eighteen cyanide ligands and fourteen coordinated water molecules (see Figure 1). The Cd (II) ions in this heterometallic compound have two different types of coordination geometry. In the first of these coordination geometries, the Cd1, Cd3 and Cd5 ions are coordinated by two nitrogen atoms from cyanide ligands and four oxygen atoms from water molecules, thus showing distorted octahedral coordination geometry.

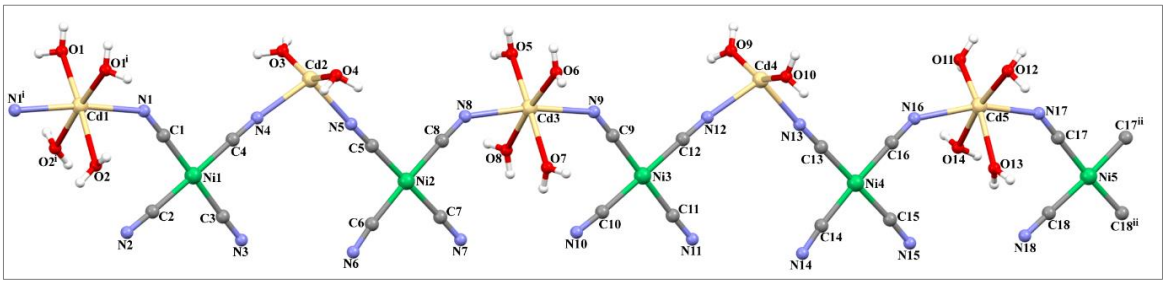

Figure 1. *The molecular structure of* ***1*** *showing the atom numbering scheme.*

In the second coordination geometry, the Cd2 and Cd4 ions are coordinated by two nitrogen atoms from cyanide ligands and two oxygen atoms from water molecules, thus showing distorted tetrahedral coordination geometry. Details of data collection and crystal structure determinations are given in Table 2. The Cd–N bond distances range between 2.209(10) and 2.442(8) Å [26-28], while the Cd–O bond distances range between 2.178(9) and 2.586(12) Å. As it can be seen in Figure 1 and Table 3, the Cd atoms and water molecules in the structure of compound **1** are sequentially bonded to each other, either double or quadruple. The bond formed when two water molecules are attached to the Cd atoms is shorter than the bond formed when four water molecules are attached to the Cd atoms. That is, the Cd atom attracts two water molecules more strongly than four water molecules. The distance between the C and N atoms in the C≡N groups in compound **1** varies between 1.12 and 1.17 Å. Depending on this situation, the bond constants of the triple bonds in the C≡N groups will also take different values. As a result of this situation, multiple splits are observed in the stretching vibrations of the C≡N group. Similar

situations are also seen between Ni-N atoms. The implications of these results will reveal the different aspects in the spectroscopic and thermal behavior of compound **1**.

Table 2 *Crystal data and structure refinement parameters for compound 1.*

Empirical formula	$C_{36}H_{56}Cd_9N_{36}Ni_9O_{28}$
Formula weight	2981.15
Crystal system	Monoclinic
Space group	*C2/c*
a (Å)	31.761 (4)
b (Å)	15.954 (2)
c (Å)	18.546 (2)
β (º)	98.379 (4)
V (Å^3)	9297.3 (19)
Z	4
D_c (g cm^{-3})	2.130
μ (mm^{-1})	3.86
θ range (º)	3.0-28.3
Measured refls.	89261
Independent refls.	8972
R_{int}	0.057
S	1.18
R1/wR2	0.077/0.163
T_{max}/T_{min}	5.92/-2.67
CCDC	1851097

Each Ni (II) ion is surrounded by four cyanide ligands, the Ni–C bond distances range between 1.842(10) and 1.883(11) Å, respectively. The coordination around Ni(II) ions are square-planar. The Cd (II) and Ni (II) ions are bridged by cyanide ligands, generating 1D coordination polymer running parallel to the [111] direction, with Cd···Ni distances ranging between 5.049 and 5.313 Å [29, 30]. The various bond types in compound **1** and the necessary information about them are given in Tables 3 and 4. Adjacent these 1D coordination polymers are further joined by O-H···N hydrogen bonds. The combination of these interactions produces 2D network (see Figure 2).

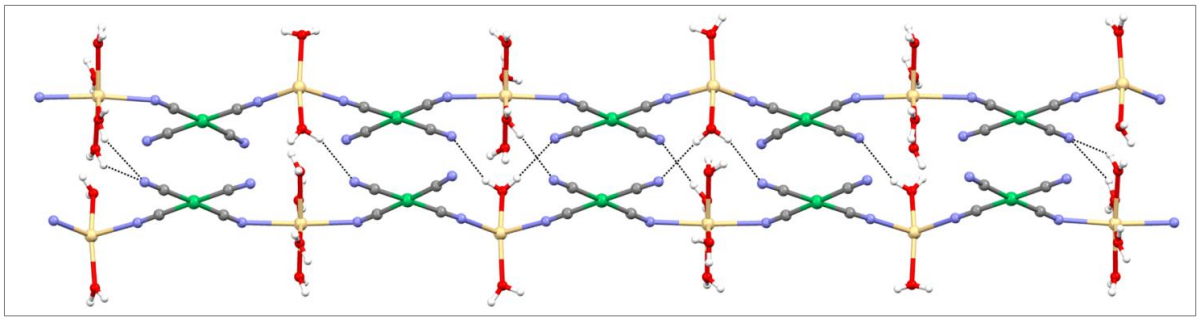

Figure 2. *An infinite 2D network in compound **1**.*

Table 3 *Selected bond distances for compound* ***1*** *(Å)*

C1-Ni1	1.853(11)	C2-Ni1	1.883(11)	C3-Ni1	1.877(11)
C4-Ni1	1.856(11)	C5-Ni2	1.863(10)	C6-Ni2	1.872(11)
C7-Ni2	1.863(11)	C8-Ni2	1.849(11)	C9-Ni3	1.863(10)
C10-Ni3	1.877(10)	C11-Ni3	1.868(11)	C12-Ni3	1.881(11)
C13-Ni4	1.867(12)	C14-Ni4	1.859(12)	C15-Ni4	1.873(11)
C16-Ni4	1.857(11)	C17-Ni5	1.842(10)	C18-Ni5	1.872(11)
Cd1-O1	2.318(9)	Cd1-O2	2.360(10)	Cd1-N1	2.420(8)
Cd2-O3	2.178(9)	Cd2-O4	2.191(9)	Cd2-N5	2.258(9)
Cd2-N4	2.291(8)	Cd3-O6	2.313(10)	Cd3-O5	2.308(9)
Cd3-O7	2.373(9)	Cd3-N8	2.375(9)	Cd3-O8	2.397(10)
Cd3-N9	2.442(8)	Cd4-O10	2.185(10)	Cd4-O9	2.185(9)
Cd4-N13	2.209(10)	Cd4-N12	2.291(9)	Cd5-O11	2.257(10)
Cd5-O12	2.282(11)	Cd5-O13	2.329(11)	Cd5-N16	2.337(9)
Cd5-O14	2.586(12)	Cd5-N17	2.375(9)		
C1-N1	1.154(13)	C2-N2	1.140(14)	C3-N3	1.124(14)
C4-N4	1.142(13)	C5-N5	1.134(13)	C6-N6	1.141(14)
C7-N7	1.146(15)	C8-N8	1.151(14)	C9-N9	1.138(13)

Table 4. *Hydrogen-bond parameters for compound* ***1*** *(Å, º)*

D-H· · ·A	D-H	H···A	D···A	D-H···A
O1—H1A···N3^{iv}	0.85	2.45	3.254 (14)	158
O1—H1B···N6^{iv}	0.84	2.45	3.274 (13)	171
O2—H2A···N3^{v}	0.88	2.59	3.461 (16)	172
O3—H3A···N7^{iv}	0.84	2.43	3.189 (14)	151
O3—H3B···N9^{vi}	0.84	2.59	3.289 (13)	142
O4—H4A···N2^{vii}	0.84	2.43	3.238 (14)	161
O4—H4B···N2^{v}	0.84	2.37	3.205 (13)	174
O5—H5A···N14^{iv}	0.84	2.61	3.305 (15)	142
O5—H5B···N11^{iv}	0.84	2.49	3.260 (14)	154
O6—H6B···N6^{vii}	0.84	2.49	3.288 (13)	160
O6—H6A···N3^{vii}	0.84	2.50	3.233 (14)	147
O7—H7A···N3^{vii}	0.97	2.58	3.495 (16)	158
O8—H8B···N11^{iv}	0.85	2.62	3.454 (15)	165
O9—H9B···N1^{vi}	0.83	2.53	3.245 (13)	146
O9—H9A···N15^{iv}	0.83	2.36	3.132 (14)	154
O10—H10B···N7^{vii}	0.84	2.50	3.178 (14)	139
O10—H10A···N10^{vii}	0.83	2.43	3.245 (14)	169
O11—H11A···N15^{iii}	0.89	2.55	3.426 (15)	174
O11—H11B···N18^{iii}	0.85	2.51	3.287 (15)	154
O12—H12B···N11^{vii}	0.81	2.49	3.193 (15)	145
O12—H12A···N14^{vii}	0.83	2.51	3.204 (16)	143
O14—H14B···N17	0.90	2.42	3.165 (18)	141
O14—H14A···O11	0.89	2.46	3.150 (18)	134

Symmetry codes: (iii) −x+2, −y+1, −z+3; (iv) x, −y+1, z−1/2; (v) −x+1, −y+1, −z; (vi) −x+3/2, −y+3/2, −z+1; (vii) x, −y+1, z+1/2.

A closer look at the smaller particles that make up compound **1** shows that these particles have two different structures. The first of these different structures is the example of a Hofmann-type-like compound formed by the Cd1 and its attached Ni $(CN)_4$ group with four water ligand molecules. The other is an example of a Hofmann-type compound formed by the Cd2 and its attached Ni $(CN)_4$ group with two water ligand molecules (see Figure 3).

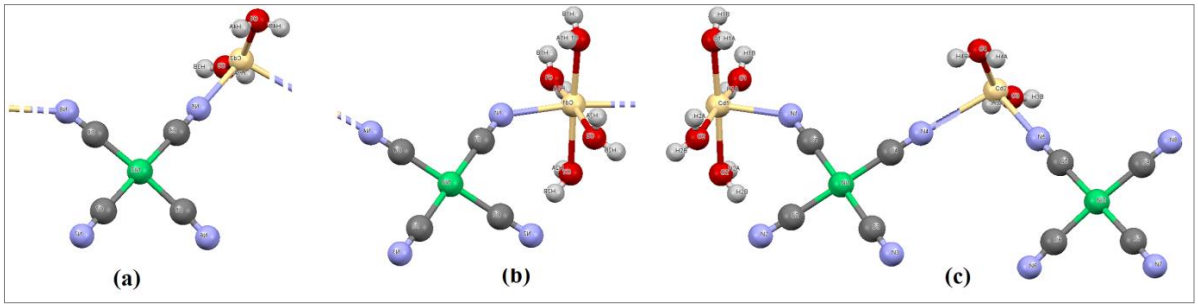

Figure 3. *Types of compounds formed by $Ni(CN)_4$ groups attached to Cd1 and Cd2 Hofmann type compound (a), Hofmann-type-like compound (b) and (c).*

As it can be clearly seen from Figure 1, the structure of compound **1** is not only in the same type. That is, it is not only in the form of a Hofmann type compound or just in the form of a Hofmann-type-like compound. The crystal structure of compound **1** consists of the sequential and regular bonding of parts (a) and (b) is shown in Figure 3. As such, the structure of compound **1** can be said to belong to the group of Hofmann-type-like compounds (Figure 3 (c)). This kind of structure is a situation that has emerged for the first time in our experimental studies. A similar structure has not been encountered in the studies of other researchers. In addition, the approximate dimensions of compound **1**'s asymmetric unit have a length of 39.30 Å and a width of 6.53 Å [in the (0bc) plane]. The approximate dimensions of a complete unit molecule in the same plane are 78.59 Å in length and 6.53 Å in width. The dimensions of the asymmetric unit of no compound we have obtained so far have not had such large values. In terms of its size values, compound **1** almost approaches the group of "supramolecules". In order to understand the structural size of compound **1**, the packed state of its crystal structure is given in Figure 4.

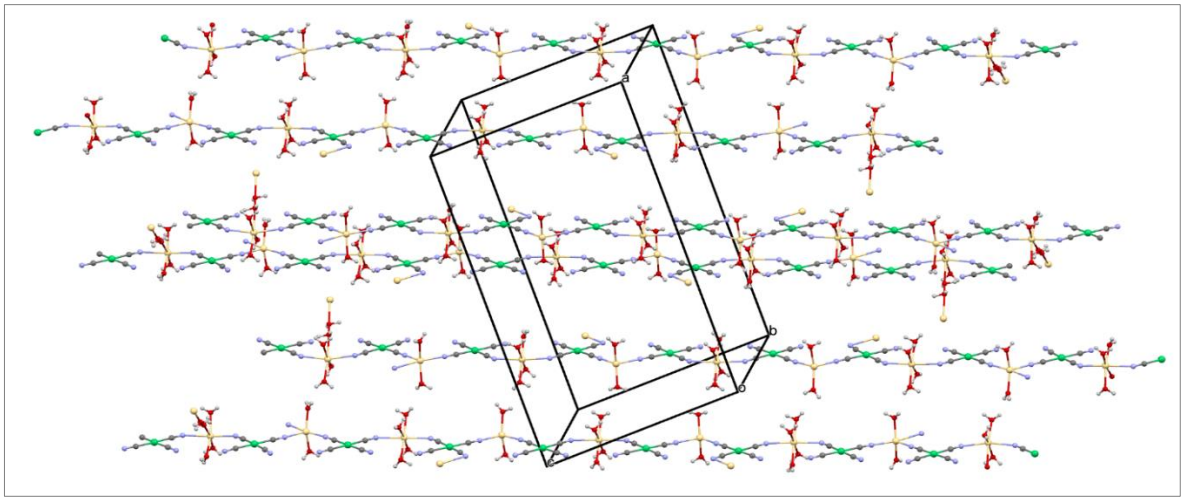

Figure 4. *The packed state of the crystal structure of compound **1**.*

Computational Studies on Compound 1

Gaussian 03 program, DFT/B3LYP method and LanL2MB basis set [31] were used in all theoretical calculations of compound **1** [32]. All the calculated values of compound **1** were made visible with the help of GaussView 4.1 program [33]. To calculate molecular geometry, atomic coordinates obtained from X-ray geometry were used. DFT calculations with a hybrid functional B3LYP (Becke's three parameters hybrid functional using the Lee-Young-Parr (LYP) correlation functional [34, 35]) using the Berny method [36, 37] were performed.

HOMO-LUMO Energy Levels of Compound 1

The HOMO and LUMO concepts of a chemical compound are defined as the "boundary orbital" of that compound. The energy difference between these boundaries orbital indicates the physical and chemical properties of that compound. In order to better understand the structure of compound **1** with some of its chemical and electronic properties, a simple model of it was made. This simple model was created from the smallest units that make up the structure of compound **1** (Figures 3 (a) and Figures 3 (b)) and their combination (Figure 3 (c)). The first part of this simple model (Figure 3 (a)) will hereinafter be referred to briefly as (**1-a**) and the second part (Figure 3 (b)) hereinafter briefly referred to as (**1-b**). Similarly, the third part (Figure 3 (c)); which is the simple model of compound **1**, hereinafter briefly referred to as (**1-c**). Some theoretical calculations have been made about each of these simple models with the Gaussian 03 program DFT/B3LYP method LanL2MB basic set [32]. In addition to these calculations, some theoretical calculations were made with the same basis set for the asymmetric part of compound **1** and for the whole. These new calculation results are hereinafter referred to as (**1-asy**) and (**1**), respectively. Theoretical calculations of all the obtained parts are listed in Table 5. These calculations were made separately for the structures in Figure 3 (a) and Figure 3 (b) and for the combined structure in Figure 3 (c). The Figure 3 (c) here is a combined form of these two simple structures, taking into account the structural symmetry of compound **1**, as an example of the main compound. Thus, it was investigated how the chemical and electronic properties of Hofmann-type compounds and Hofmann-type-like compounds change as a result of the combination of these compounds. The boundary orbitals of simple models assumed to contribute to the formation of compound **1** and compound **1** are given in Figure 5 and Figure 6, respectively.

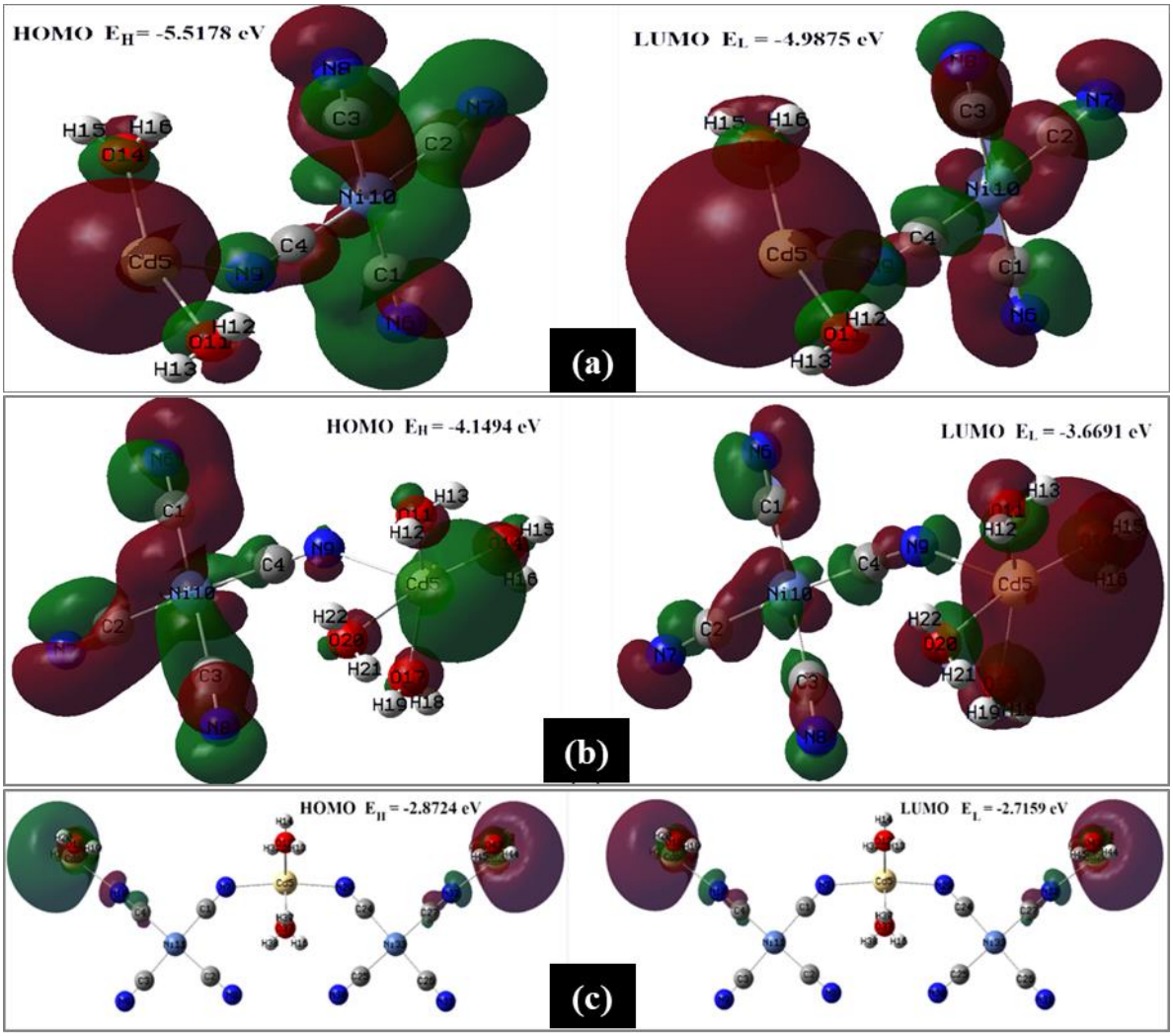

Figure 5. *According to the DFT/B3LYP method and the LanL2MB basis set, the graphics of boundary orbitals of the theoretical units of compound 1 (a) and (b) and of their combinations (c).*

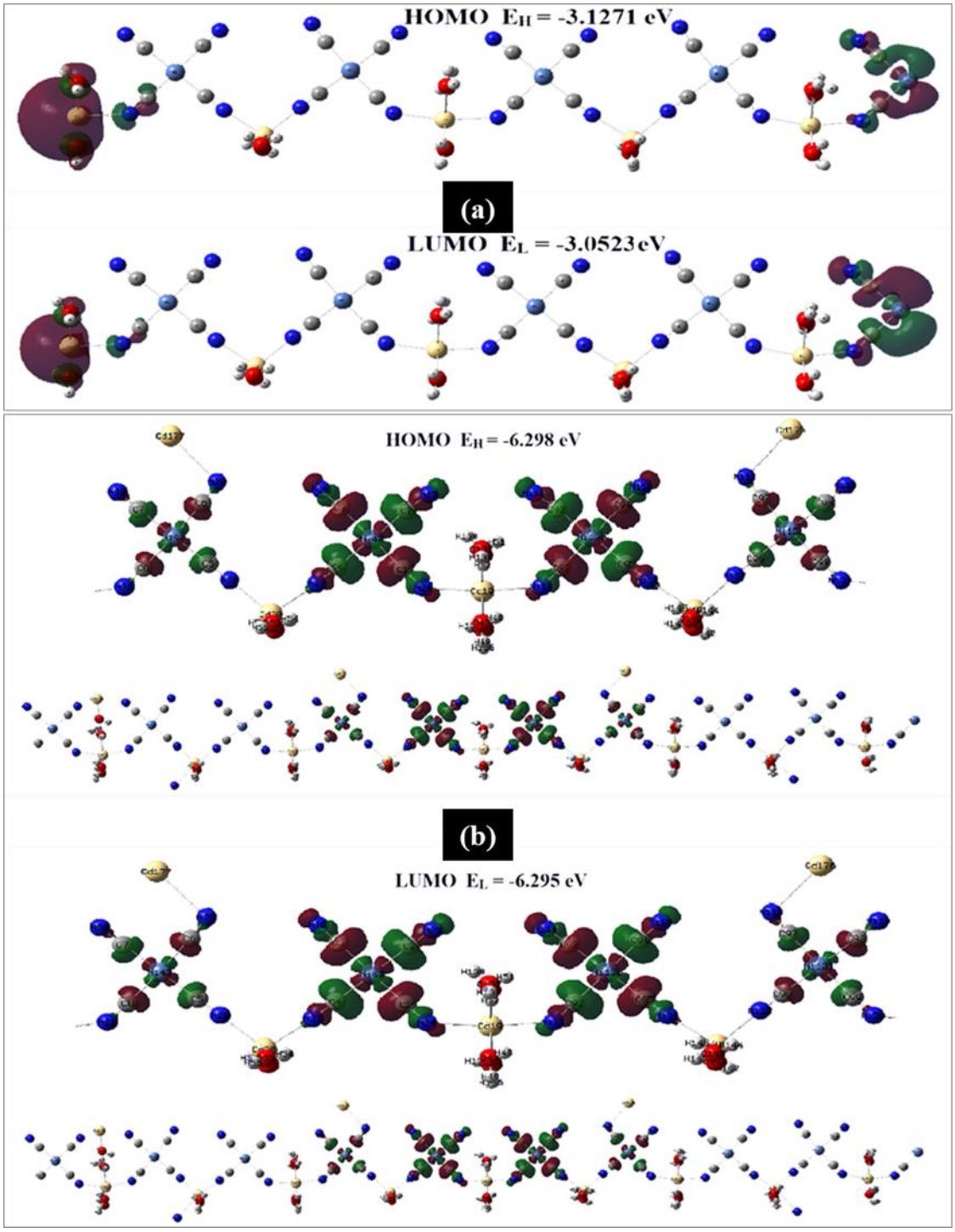

Figure 6. *Also, the graphics of boundary orbitals of the asymmetric unit of experimental compound* ***1*** *(a) and of all experimental compound* ***1*** *(b).*

On closer inspection of Figure 5, it can be seen that in simple models of compound **1** with few atoms, the boundary orbitals are distributed over almost all atoms (see Figure 5 (a) and Figure 5 (b)). In Figure 5 (c) and Figure 6 (a), it is seen that the boundary orbitals prefer to be located at the ends of the structure in structures with more atoms. It is seen that the boundary orbitals of compound **1** are located on the $[Ni(CN)_4]^2$ ion groups located in the middle of the structure (see Figure 6 (b)). They have been re-inserted into this figure at greater magnification to give a better view of the boundary orbitals. The following

conclusion can be drawn from this: the shape and arrangement of the boundary orbitals in a compound are closely related to the number of atoms and ion groups in that compound and to their arrangement with respect to each other. The occupied orbital, vacant orbital, total orbital numbers and HOMO, LUMO values of the compounds and some chemical efficiency values are given in Table 5.

The electronic properties of a compound obtained by chemical methods are calculated with the help of its ionization potential (I = -HOMO) and Electron affinity (A = -LUMO) values. The formulae for some parameters that can be calculated with the help of the ionization potential (I) and electron affinity (A) values of a compound are listed below [38-41].

$\Delta E = A - I$ (Energy gap value) (1)

$\chi = (I + A) / 2 = -\mu$ (Electronegativity, Negative chemical potential) (2)

$\eta = (I - A) / 2$ (Chemical hardness) (3)

$S = 1 / 2\eta$ (Chemical softness) (4)

$\omega = \mu^2 / 2\eta$ (Electrophilicity index) (5)

The energy gap value (ΔE), electronegativity (χ), negative chemical potential (-μ), chemical hardness (η), chemical softness (S) and electrophilicity index values (ω) calculated for all compounds according to these formulae are given in Table 5 in term (eV) unit.

Table 5 *Calculated frontier molecular orbitals energies and chemical reactivity descriptors (in "eV" units)*

Chemical efficiency values	**Compounds**				
	1-a	**1-b**	**1-c**	**1-asy**	**1**
Occupied orbital	51	61	128	262	550
Vacant orbital	25	29	61	126	264
Total orbital	76	90	189	388	814
HOMO (-I)	-5.5178	-4.1494	-2.8724	-3.1271	-6.298
LUMO (-A)	-4.9875	-3.6691	-2.7159	-3.0523	-6.295
ΔE = (A – I)	0.5303	0.4803	0,1565	0.0748	0.00272
χ	5.2527	3.9093	2.7942	3.0897	6.2966
μ	-5.2527	-3.9093	-2.7942	-3.0897	-6.2966
η	0.2652	0.2402	0.0783	0.0374	0.00136
S $(eV)^{-1}$	1.8854	2.0816	6.3898	13.3690	367.647
ω	34.0983	31.8123	49.8885	127.6238	14570.376

After examining the theoretical values in Table 5, the following conclusions can be reached:

- The number of occupied, vacant and total orbital in a compound increases in direct proportion to the number of atoms in that compound.
- The difference between HOMO and LUMO energy levels in a compound is inversely proportional to the number of atoms in that compound.
- The values of HOMO and LUMO energy levels in a compound depend more on the type of atoms and the arrangement of those atoms than on the number of atoms in that compound.

- While the η value of a compound is inversely proportional to the number of atoms in that compound, the S and ω values are generally directly proportional to the number of atoms in that compound.

Calculations of Some Other Chemical Properties of Compound 1 and Its Theoretical Representatives

The electric dipole moment of a compound composed of different atoms and molecules is due to the molecular charge distribution of that compound. The electric dipole moment of a compound has a 3D vector character in 3D space. Therefore, the electric dipole moment can be used to show the motion of electric charges in a compound. The orientation of the dipole moment vector in a compound in 3D space depends on the location of the centers of the positive and negative charges in that compound. The dipole moment of a compound in electrostatic equilibrium is constant and its positioning is precisely determined. If an external electric field is applied to the electron cloud of any compound in electrostatic equilibrium, its electric charges will move and its charge balance will be disturbed. This degree of distribution is called "polarizability" for that compound. Often, the term "polarizability" is used instead of the term "mean polarizability". The electric dipole moments (μ), average polarizability (α_0), polarizability anisotropies (Δα) and first-order hyperpolarizability (β_0) values of the asymmetric part of compound **1** and its theoretical representatives were calculated by the finite field method using the LanL2MB basis set in DFT/B3LYP [31, 32]. When trying to calculate the μ, α_0, Δα and β_0 values of all of compound **1** with the same method, a negative result was always encountered. This negative result is thought to be due to the fact that the structure of compound **1** is too large to be resolved by the calculation method used. The formulae used to obtain the amounts of (μ), (α_0), (Δα) and (β_0) specific values of these compounds are given below, respectively. These formulae have been used by many researchers and us before [42-44].

$$\mu = \sqrt{\mu_x^2 + \mu_y^2 + \mu_z^2} \quad \text{(Dipole moment)} \tag{6}$$

$$\alpha_0 = \frac{\alpha_{xx}+\alpha_{yy}+\alpha_{zz}}{3} \quad \text{(Mean polarizability)} \tag{7}$$

$$\Delta\alpha = \sqrt{\frac{(\alpha_{xx}-\alpha_{yy})^2+(\alpha_{yy}-\alpha_{zz})^2+(\alpha_{zz}-\alpha_{xx})^2+6(\alpha_{xy}^2+\alpha_{xz}^2+\alpha_{zy}^2)}{2}} \quad \text{(Anisotropies of polarizability)} \tag{8}$$

$$\beta_0 = \sqrt{\beta_x^2 + \beta_y^2 + \beta_z^2} \quad \text{(First-order hyperpolarizability)} \tag{9}$$

$$\beta_x = \beta_{xxx} + \beta_{xyy} + \beta_{xzz} \quad \text{(x component of } \beta_0\text{)} \tag{10}$$

$$\beta_y = \beta_{yyy} + \beta_{xxy} + \beta_{yzz} \quad \text{(y component of } \beta_0\text{)} \tag{11}$$

$$\beta_z = \beta_{zzz} + \beta_{xxz} + \beta_{yyz} \quad \text{(z component of } \beta_0\text{)} \tag{12}$$

The calculated (μ), (α_0), (Δα) and (β_0) values of the compounds using these formulae are given in Table 6. In this study, the theoretically calculated $\Delta\alpha$, α_0 and β_0 values for the compounds were converted

from atomic units (au) to electrostatic units (esu) with the factors of 0.1482×10^{-24} and 8.6393×10^{-33}, respectively. [42, 43].

***Table 6**. The μ, α_0, Δα and β_0 values of the asymmetric part of compound **1** and its theoretical representatives*

Parameters	Compounds			
	1-a	**1-b**	**1-c**	**1-asy**
μ_x (D)	-24.6654	35.6274	0.0643	73.8146
μ_y (D)	2.2919	-4.6636	38.7170	-78.5181
μ_z (D)	1.2564	1.8401	0.8494	0.8494
μ (D)	24.8035	35.9785	38.7264	107.7668
α_{xx} (au)	-89.1973	-107.8012	-169.8287	-22.7458
α_{xy} (au)	2.6674	-0.5592	-0.1760	6.4194
α_{yy} (au)	-92.7932	-111.7138	-274.7731	-479.5327
α_{xz} (au)	-11.1955	3.7203	-14.1062	12.7070
α_{yz} (au)	-14.4335	1.2258	0.3310	27.5447
α_{zz} (au)	-78.0362	-69.5888	-129.9467	-301.9711
Δα (esu)	5.1337×10^{-24}	6.0582×10^{-24}	1.9203×10^{-23}	5.9642×10^{-23}
α_0 (esu)	-3.8536×10^{-23}	-4.2845×10^{-23}	-2.8383×10^{-23}	-3.973×10^{-23}
β_{xxx} (au)	-526.5466	734.0383	4.3061	22328.6763
β_{xxy} (au)	-33.5952	27.0237	1207.2505	-8235.3116
β_{xyy} (au)	-153.5749	179.2955	-0.7505	383.2087
β_{yyy} (a.u.)	43.5007	-51.1417	701.2097	-1473.0625
β_{xxz} (au)	49.8452	15.6047	40.8439	-85.3687
β_{xyz} (au)	10.3340	0.4362	-94.1506	-262.8113
β_{yyz} (au)	-14.7025	-3.5084	3.5014	-32.2804
β_{xzz} (au)	-96.4647	149.0481	-0.1803	-47.8405
β_{yzz} (au)	1.7828	-24.1799	202.3563	-374.1381
β_{zzz} (au)	3.5123	15.8444	4.1633	4.6113
β_0 (esu)	6.7182×10^{-30}	7.9053×10^{-30}	1.0438×10^{-29}	2.0946×10^{-28}

According to the analysis made on the values in Table 6, the following results were obtained.

- The dipole moment values of the studied theoretical and experimental compounds are directly proportional to their atomic number, that is, to their electric charge.
- Since α_0 and Δα values of the studied theoretical and experimental compounds depend on the distribution of their atoms and electric charges in 3D space, there is no certain proportionality between these values.
- The β_0 values of the studied theoretical and experimental compounds are equal to the square root of the sum of the squares of their β_x, β_y and β_z components. In other words, these values are increasing in direct proportion to the number of atoms in the compounds and their electrical charges.

Hirshfeld Surface Analysis of Compound 1

Types of bonds that ensure the stability of a crystalline structure; They are in the form of metallic bonds, various types of bonds between other atoms in the structure, hydrogen-hydrogen and van der Walls interactions of smaller intensity. A program called CrystalExplorer was created by Spackman et al to calculate weak interactions in crystal structures [45]. This program can calculate the surface types of a

crystal such as Hirshfeld, Promolecule, Crystal Voids, Electron Density, Deformation Density, Electrostatic Potentials, Molecular Orbitals and Spin Density [45]. A 2D map of the Hirshfeld surface calculated for a molecular structure is very important in understanding the intramolecular interactions of that molecular structure. Hirshfeld surface analysis, which is used to identify various interactions in a crystal structure, identifies these interactions with the help of red, blue and white colors. Red areas on a Hirshfeld surface indicate hydrogen bond interactions, blue areas indicate long-reach interactions, and white areas indicate van der Waals interactions. The intensity of each color on the Hirshfeld surface of a crystal structure is directly proportional to the magnitude of the interactions [45]. The Hirshfeld surface analysis approach of compound **1** is a graph-based tool that facilitates understanding interactions in that molecular structure [45]. The different views of the Hirshfeld surface created by the CrystalExplorer program for compound **1** and the 2D fingerprint graphs produced from them and the percentages of various interactions are shown in Figure 7.

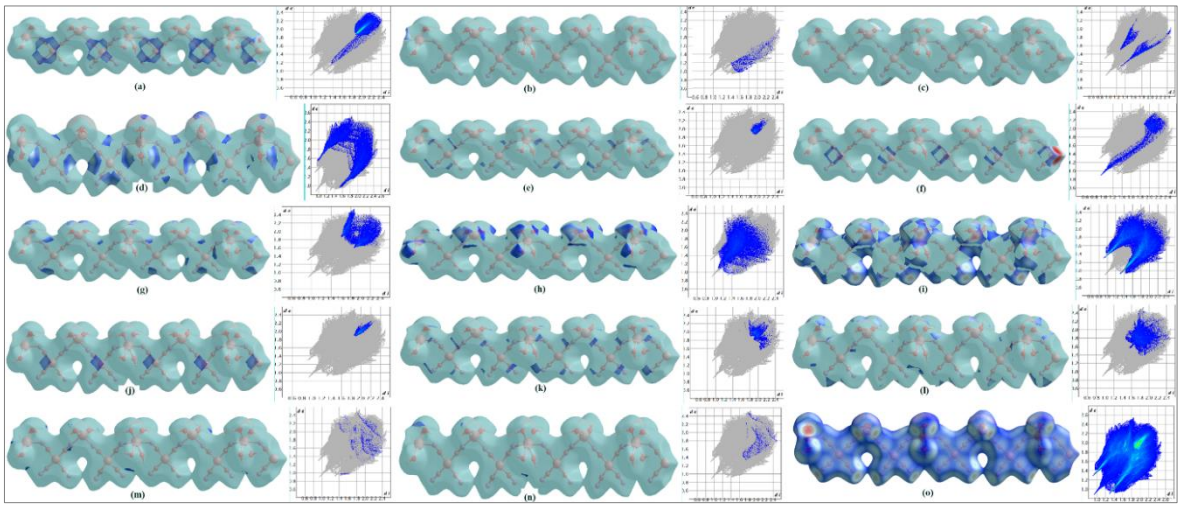

Figure 7. *Percentages of contribution of some intramolecular and extramolecular interactions in the asymmetric part of compound* ***1*** *to crystal formation; C…C (a), Cd…H/H…Cd (b), Cd…N/N…Cd (c), C…H/H…C (d), C…N/N…C (e), C…Ni/Ni…C (f), C…O/O…C (g), H…H (h), N…H/H…N (I), Ni…Ni (j), N…N (k), N…O/O…N (l), O…H/H…O (m), O…O (n), and 2D fingerprint plot of all interactions in the asymmetric part of compound* ***1*** *(o)*

A 2D fingerprint graph of a crystal structure makes it possible to quantitatively examine all the molecular interactions in that crystal structure together. The 2D fingerprint graph provides the advantage of highlighting and distinguishing short-range contacts in the crystalline structure [45]. From all the 2D fingerprint views of compound **1**, the interactions that hold the molecules together in its crystal structure are N-H, C-H, C-C, H-H, C-C, C-O, N-O, C-Ni, N-N, Cd-N, N-N, Ni-Ni … and others. The contributions of these interactions to the formation of the crystal structure of compound **1** are shown in Table 7.

Tablo 7. *The contribution percentages of each of the intramolecular and intermolecular interactions that form the crystal structure in the asymmetric part of compound **1** to the Hirshfeld surfaces, ordered from largest to smallest.*

Interactions	Contribution (%)
N--H/H--N	40.8
H--H	12.4
C--H/H--C	10.3
C--C	8.3
C--O/O--C	6.5
N--O/O--N	6.4
C--Ni/Ni--C	3.2
N--N	2.7
Cd--N/N--Cd	2.6
Ni--Ni	2.2
C--N/N--C	1.3
Cd--O/O--Cd	0.9
O--H/H--O	0.7
O--O	0.6
Cd--H/H--Cd	0.5

Interpretation of The FT-IR Spectrum of Compound 1

Experimental FT-IR spectrum of compound **1** is given in Figure 8. In this spectrum, firstly, the vibration modes of the water molecule, which is the ligand, and then the $[Ni(CN)_4]^{2-}$ ion group were investigated separately.

Vibrations of the H_2O in Compound 1

Since there are two hydrogen and one oxygen atoms in the structure of the water molecule, it has three vibration modes defined as νas(OH), νs(OH) and δ(OH) in its FT-IR spectrum [46 - 48]. A new vibration band is formed as a result of the overlapping of νas(OH) and νs(OH) modes in the FT-IR spectrum of the compound formed by bonding a water molecule to a metal atom. This new vibration band belongs to the water molecule and is a very broad band in the range of wavenumbers of about 3500 and 3200 cm-1. If a compound has unbounded water molecules in its structure, then in its FT-IR spectrum, a single very sharp and intense stretching vibration peak appears around the wavenumber of 3600 cm-1. However, in some cases, in the FT-IR spectra of aqueous compounds with bound water molecules, the vibration modes νas(OH) and νs(OH) can be seen separately at lower wavenumbers than in the free water molecule. The vibration modes of liquid water were experimentally obtained in our laboratory at wavenumbers ν_{as}(OH) 3470 cm^{-1}, ν_s(OH) 3257 cm^{-1} and δ(OH) 1641 cm^{-1}. As can be easily seen from all the figures of the crystal structure of compound **1**, the water molecules are attached to the Cd atoms as two different groups. The physical conditions are different for the bound water molecule in each different group. Therefore, at least two different vibration groups should be expected for the bound water molecules. In fact, in the same region, peaks belonging to the combination and overtones of some of the vibration modes formed at lower wavenumbers of the H_2O molecule and the $[Ni(CN)_4]^{2-}$ ion group can

be found.

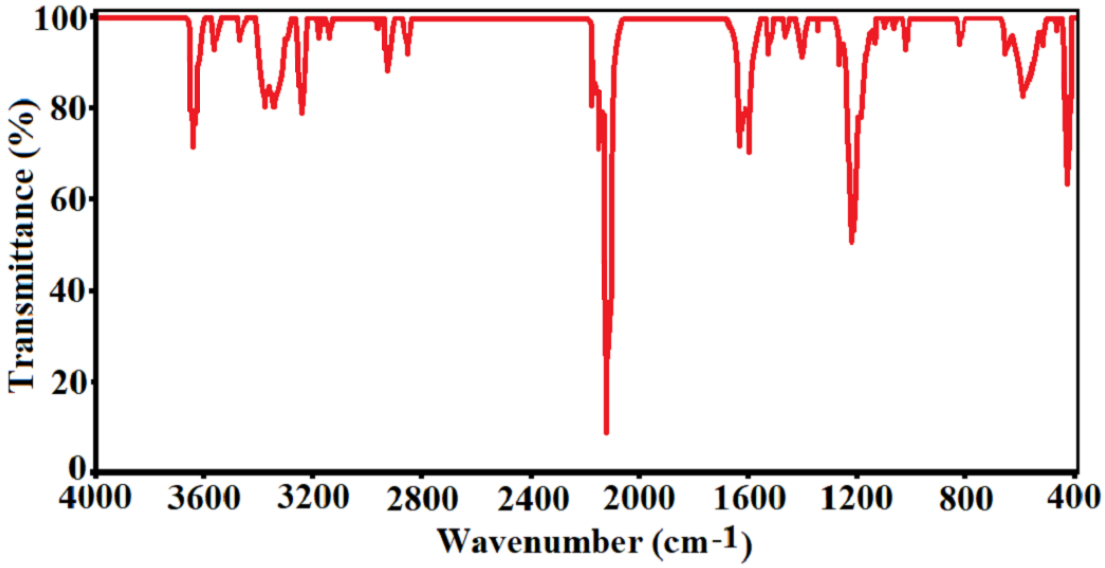

Figure 8*. The experimental FT-IR spectra of compound* ***1****.*

It is a fact that water molecules bonded to Cd atoms as binary groups will be under the influence of a stronger attraction force by the Cd atom than water molecules bonded as quaternary groups. As a result of this situation, the vibrations found in the higher wavenumber will belong to the water molecules that are bonded in binary. From the FT-IR spectrum of compound **1**, values of 3567 and 3373 cm^{-1} with 3548 and 3346 cm^{-1} can be assigned for ν_{as}(OH) and ν_{s}(OH) vibrations for binary and quaternary H_2O groups, respectively. From these results, it was seen that the ν_{as}(OH) and ν_{s}(OH) vibration modes of the binary and quaternary H_2O groups in compound **1** shifted to higher wavenumbers compared to the values of the vibrations in the liquid water molecule. The shift values to this high wavenumber are (97 - 78) cm^{-1} and (116 - 89) cm^{-1}, respectively. The vibration peak seen at wave number 3643 cm^{-1} in the FT-IR spectrum of compound **1** indicates that some water molecules are guests in the cavities of the crystal structure, without binding to any atoms. However, there is no water molecule as a guest in the crystal structure of compound **1**, which was resolved by the SC-XRD method. The explanation for this is when compound **1** first formed; its immediate FT-IR spectrum was taken. At that moment, there are some guest water molecules in compound **1**. However, about six months after obtaining compound **1**, its crystal structure was resolved and its elemental analysis was carried out. During this long period of time, the guest water molecules were separated from the crystal structure of compound **1**. The two peaks observed at wavenumbers 1625 and 1602 cm^{-1} in the FT-IR spectrum of compound **1** in Figure 4 correspond to the bending vibrations of the two different water groups in compound **1**. These bending vibrations shifted to the wavenumber region as low as 16 and 39 cm^{-1} value relative to the values in the free water molecule.

Vibrations of the $[Ni(CN)_4]^{2-}$ Ion Group in Compound 1

Various theoretical and experimental information about the $[Ni(CN)_4]^{2-}$ ion group can be seen in

previous articles of ours and other researchers [6, 7, 9-19, 45, 46]. The vibration modes of the [Ni $(CN)_4]^{2-}$ ion in the $K_2[Ni(CN)_4]\cdot H_2O$ compound and the vibration modes of the $[Ni(CN)_4]^{2-}$ ion in the compound **1**'s structure were compared with each other. In this way, the effect of compound formation on these modes was investigated. In the FT-IR spectrum of a compound with a cyanide group, sharp peaks with varying intensity in the wavenumber range of 2200-2000 cm^{-1} correspond to cyanide groups [20, 46]. The study of McCullough et al on this subject was used to determine the vibration modes of the [Ni $(CN)_4]^{2-}$ ion in compound **1** [50]. Let us examine the most important vibration modes of $K_2[Ni(CN)_4]\cdot H_2O$ in order from largest wavenumber to smallest. In the FT-IR spectrum of $K_2[Ni(CN)_4]\cdot H_2O$, the ν_8(Ni–CN), E_u mode is at 2122 cm^{-1}. This vibration mode was observed in compound **1** at wavenumbers 2168, 2145, and 2123 cm^{-1} as splitting into three. The reason for this triple splitting can be understood by examining the crystal structure of compound **1**. The nitrogen atoms of the four cyan groups in the structure of compound 1 form three different bonding patterns with other atoms around it. These bonding forms are the bond between N and two different H atoms, the bond between N and Cd atoms, and the bond between N and Cd and H atoms, respectively. It can be said that the bond constants of these bonds are in the same order of magnitude but at different values close to each other. These three types of bonds with different bond constants cause the vibration mode of the cyan group to be split into three. It can be said that ν_9(Ni–CN), E_u; π(Ni–CN), A_{2u} and δ(Ni–CN), E_u vibration modes appear in the FT-IR spectrum of compound **1** at wavenumbers of 584, 462 and 420 cm^{-1}. However, in the FT-IR spectrum of compound **1**, it is very difficult to accurately interpret the peak values in this region. Because, in this region, stretching and bending vibrations of CN groups with three different properties and various modes of some other groups coexist.

Thermal Behavior of the Compound 1

TGA and DTG graphs of compound **1** are given in Figure 9. According to his TGA graph, compound **1** preserved its crystalline structure while heating from 20 °C to 90 °C. However, after this temperature, water molecules, which are ligands, started to separate from the crystal structure of compound **1**. In this first step of the thermal analysis, 4 water molecules attached to the Cd atom left the crystal structure of compound **1**. These 4 water molecules were first separated from the crystal structure of compound **1** because they have weaker bonds than the 2 water molecules attached to the other Cd atom. This first step of the thermal analysis occurred in the low temperature range of 90 - 116 °C, with a peak of about 105 °C. [found/(calc.)% = 11.85/(12.09)%].

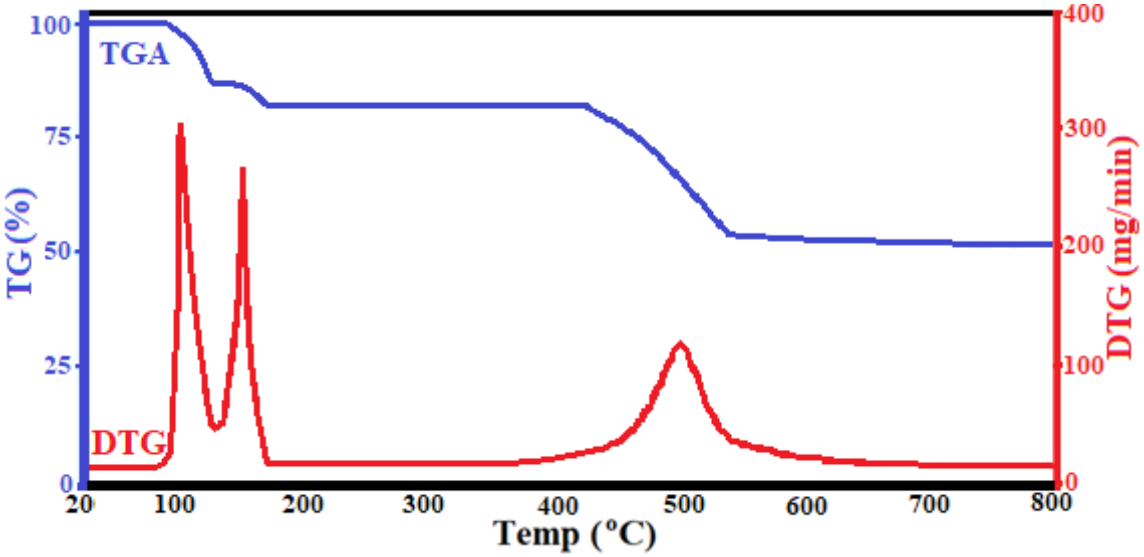

Figure 9*. Thermal graphic of compound **1**.*

In the second step of the thermal analysis of compound **1**, 2 water molecules, which were more tightly bound as ligands to the other Cd atom in the crystal structure, were separated from the crystal structure of compound **1**. This second step of the thermal analysis took place in the temperature range 125–180 °C, which is a slightly higher temperature range than the first temperature range, with a peak at 158 °C. [found/(calc.)% = 4.48/(4.84) %]. In the third step of the thermal analysis, it is thought that the square planar $Ni(CN)_4$ bridges in the structure of compound **1** deteriorate with the effect of increasing temperature. In this step, the triple bonds in the CN groups were broken, and then the C and N atoms were burned out by the effect of high temperature. It can be seen from Figure 9 that the third step of the thermal analysis occurs in the temperature range of about 442–544 °C and has a peak at 497 °C. [found/(calc.) % = 30.87/(31.43) %]. Finally, it is understood that only Cd and Ni atoms remained in the thermal analysis of compound **1**. [found/(calculated)% = 51.18/(51.66)%].

Conclusion

In this study, a new heterometallic Hofmann-type-like compound defined by the open formula $[Cd(H_2O)_2Ni(CN)_4]_4[Cd(H_2O)_4Ni(CN)_4]_5$ was synthesized in crystal form by chemical reaction. In the reaction medium, water was used both as a ligand molecule and as a solvent. In this heterometallic new Hofmann-type-like compound, the H_2O ligand molecule behaved like a monodentate ligand molecule by binding from the O atom to the Cd transition metal atoms. These Cd-O bonds played a very important role in the formation and stability of the crystal structure of the obtained new heterometallic compound **1**. In obtaining the crystal structure of compound **1**, the bonds made by the oxygen atom of the ligand water molecule with the Cd transition metal atom, as well as the various bonds made by its hydrogen atoms with different atoms in the environment played very important roles. The various bonds that the hydrogen atoms of the ligand water molecule make with different atoms in the environment show a distribution ranging from the strongest to the weakest bonds forming the crystal structure of compound

1 (see Table 7). In addition, due to the weak interaction forces between the ligand water molecules forming the structure of compound **1**, it was thought that its volume could easily change depending on the guest molecules that would enter this structure. Therefore, the volumes of the host structures formed by the ligand water molecule will be able to stretch at a certain rate. Therefore, it can be thought that these new structures are more suitable for the storage of certain gases and other guest molecules than the host structures formed by larger ligand molecules. Furthermore, all Ni (II) ions in the structure of the crystal of compound 1 are surrounded by four cyanide groups, forming a square planar arrangement. In contrast, Cd (II) ions possess two distinct environmental arrangements within the structure. In one of these coordination geometries, some Cd (II) ions have a distorted octahedral coordination geometry formed by the two nitrogen atoms of the cyanide groups and the four oxygen atoms of the ligand water molecules. In the other coordination geometry, the other Cd (II) ions have a distorted tetrahedral coordination geometry formed by the two nitrogen atoms of the cyanide groups and the two oxygen atoms of the ligand water molecules. The probabilities of various guest molecules of suitable size entering the gaps in the structure of compound **1**, which is a Hofmann-type-like compound obtained in crystalline form, can be investigated experimentally. Consequently, clathrate forms of compound **1** can be obtained in future studies.

Acknowledgement -

Funding/Financial Disclosure The authors wish to thank in particular Kütahya Dumlupınar University, Türkiye, for the technical [Department of Physics and Chemistry; Advanced Technologies Center (İLTEM)] and financial support with the project number 2017/25.

Ethics Committee Approval and Permissions The study does not require ethics committee approval or any special permission.

Conflicts of Interest The authors declare that they have no known competing financial interests or personal relationships that could have appeared to influence the work reported in this paper.

Authors Contribution Authors contributed equally to the work.

References

[1] OpenStax, Chemistry. OpenStax CNX. Jun 20, 2016 http://cnx.org/contents/85abf193-2bd2-4908-8563-90b8a7ac8df6@9.311.

[2] The Materials Project (2020). Materials Data on $K_2Ni(CN)_4$ by Materials Project. United States. https://doi.org/10.17188/1307699

[3] Hofmann, K. A. & Küspert, F. (1897). Verbindungen von kohlenwasserstoffen mit metallsalzen. *Zeitschrift Für Anorganische Chemie, 15(1),* 204-207. http:/doi.org/10.1002/zaac.18970150118

[4] Hagan, M. (1962). *Clathrate Inclusion Compounds.* Reinhold Publishing Corporation, Chapman & Hall Ltd., New York. p. 5.

[5] Iwamoto, T. (1984). Inclusion Compounds, Vol. 1, Chapter 2 (Eds. J. L. Atwood, J. E. D. Davies, and D. D. MacNicol). Academic Press, London, p. 29.

[6] Türköz, D., Kartal, Z., & Bahçeli, S. (2004). Ft-Ir Spectroscopic Study Of Co(1-Propanethiol)$_2$Ni(CN)$_4$·Benzene Clathrate. *Zeitschrift Für Naturforschung A*, *59*, 7-8. http:/doi.org/10.1515/zna-2004-7-819

[7] Kartal, Z. (2005). IR spectroscopic study of M (benzoic acid)$_2$Ni(CN)$_4$.(1,4-dioxane) clathrate (M = Ni, Cd and Co). *Zeitschrift für Naturforschung A*, *60*(A), 469-472. http:/doi.org/10.1515/zna-2005-0613

[8] Kartal, Z., Parlak, C., Şentürk, Ş., Aytekin, M. T. & Şenyel, M. (2007). FT-IR Spectroscopic Study of the Hofmann-Td-type Clathrates: Ni(1,9- diaminononane)M′(CN)$_4$·2G (M′ = Cd or Hg, G = Benzene, 1,2-Dichlorobenzene or 1,4-Dichlorobenzene). *Croatica Chemica Acta*, *80*(1), 9-15. https://hrcak.srce.hr/12805

[9] Kartal, Z. (2009). FT-IR spectroscopic study on some Hofmann-type clathrates: M(p-Benzoquinone)Ni(CN)$_4$·2G (M = Mn, Co, Ni or Hg; G = Aniline). *Journal of Molecular Structure*, *938*(1-3), 70–75. http:/doi.org/10.1016/j.molstruc.2009.09.005

[10] Kartal, Z. & Sayın, E. (2011). FTIR spectroscopic and thermal study of M(Cyclohexanethiol)$_2$Ni(CN)$_4$.(1,4-dioxane) clathrate (M = Mn, Co, Ni and Cd). *Journal of Molecular Structure*, *994*, 170-178. http:/doi.org/10.1016/j.molstruc.2011.03.014

[11] Kartal, Z. (2012). Vibrational spectroscopic investigation on some M(Benzonitrile)$_2$Ni(CN)$_4$ complexes (M = Ni, Zn, Cd and Hg). *Brazilian Journal of Physics*, *42*, 6-13. http:/doi.org/10.1007/s13538-011-0054-x

[12] Kartal, Z. & Türk, T. (2021). FT-IR spectroscopic and thermal study of M(1,6-hexanedithiol) Ni(CN)$_4$.2(1,4-dioxane) clathrate(M = Mn, Co, Ni and Cd). *Journal of Molecular Structure, 1014*, 74-80. http:/doi.org/10.1016/j.molstruc.2012.01.031

[13] Kartal, Z. (2016). Synthesis, spectroscopic, thermal and structural properties of [M(3-aminopyridine)$_2$Ni(μ-CN)$_2$(CN)$_2$]$_n$ [M(II) = Co and Cu] heteropolynuclear cyano-bridged complexes. *Spectrochimica Acta Part A: Molecular and Biomolecular Spectroscopy*, *152*, 577–583. http:/doi.org/10.1016/j.saa.2014.12.117

[14] Kartal, Z. & Yavuz, A. (2018). The synthesis and the spectroscopic, thermal, and structural properties of the M$_2$[(fumarate)Ni(CN)$_4$].2(1,4-dioxane) clathrate (M = Co, Ni, Cd and Hg). *Journal of Molecular Structure*, *1155*, 171-183. http:/doi.org/ 10.1016/j.molstruc.2017.10.107

[15] Kartal, Z., Şahin, O. & Yavuz, A. (2018). The synthesis of two new Hofmann-type M(3-aminopyridine)$_2$Ni(CN)$_4$ [M = Zn(II)and Cd(II)] complexes and the characterization of their crystal structure by various spectroscopic methods. *Journal of Molecular Structure, 1171*, 578-586. http:/doi.org/10.1016/j.molstruc.2018.06.042

[16] Kartal, Z. & Şahin, O. (2021). Synthesis, spectroscopic, thermal, crystal structure prop- erties and characterization of new Hofmann-type-like clathrates with 4-aminopyridine and water. *Turkish Journal of Chemistry, 45*, 616–633. http:/doi.org/10.3906/ kim- 2011- 29

[17] Kartal, Z. & Şahin, O. (2021). Synthesis, spectroscopic, thermal, crystal structure prop- erties, and characterization of new Hofmann-T$_d$-type complexes with 3- aminopyridine, *Turkish. Journal of Chemistry, 45*, 942–955. http:/doi.org/10.3906/kim-2101-32

[18] Kartal, Z., Şahin, O. & Yavuz, A. (2019). Synthesis of Hofmann-type $Zn(H_2O)_2Ni(CN)_4.nG$ (G = water and 1,4-dioxane) clathrates and the determination of their structural properties by various spectroscopic methods, *Turkish Journal of Chemistry*, *43(6)*, 1608–1621. http:/doi.org/10.3906/kim-1906-26

[19] Kartal, Z. & Şahin, O. (2022). Synthesis of two Hofmann type and Hofmann-type-like compounds in crystal form from 4-aminopyridine and their characterizations by various methods. *Journal of Molecular Structure*, *1252*, 132088. https://doi.org/10.1016/j.molstruc.2021.132088.

[20] Nakamoto, K. (2009). *Infrared and Raman Spectra of Inorganic and Coordination Compounds, Part B, Applications in coordination, organometallic, and bioinorganic chemistry,* John Wiley and Sons, Hoboken, New Jersey.

[21] Smékal, Z., Císařová, I. & Mroziński, J. (2001). Cyano-bridged bimetallic complexes of copper(II) with tetracyanonickelate(II). Crystal structure of $[Cu(dpt)Ni(CN)_4]$. *Polyhedron*, *20*, 3301–3306.http:/ doi.org/10.1016/S0277-5387(01)00942-1

[22] Sheldrick, G. M. (2008). A short history of SHELX. *Acta Crystallographica*, *A64*,112-122. https://doi.org/10.1107/S0108767307043930.

[23] Sheldrick, G. M. (2015). Crystal structure refinement with SHELXL. *Acta Crystallographica*, *C71*, 3-8. http://dx.doi.org/10.1107/S2053229614024218

[24] APEX2, Bruker AXS Inc. Madison Wisconsin USA (2013).

[25] Macrae, C. F., Sovago, I., Cottrell, S. J., Galek, P. T. A., McCabe, P., Pidcock, E., Platings, M., Shields, G. P., Stevens, J. S., Towler, M. & Wood, P. A. (2020). Mercury 4.0: from visualization to analysis, design and prediction. *Journal of Applied. Crystalography*, *53*, 226-235. https://doi.org/10.1107/S1600576719014092

[26] Şenocak, A., Karadağ, A., Soylu, M. S. & Andac, O. (2015). Two novel cyanido-bridged polymeric complexes with suspension bridge type connections and a series of related complex salts: crystallographic and thermal characterizations. *New Journal of Chemistry*, *39(5)*, 3675-3686. https://doi.org/10.1039/C5NJ00071H

[27] Kurkcuoglu, G. S., Hokelek, T., Aksel, M., Yesilel, O. Z. & Dal, H. (2011). Cyano-Bridged Heteropolynuclear Ni(II), Cu(II) and Cd(II) Complexes, [M(deten) Ni(μ-CN) (CN)]. *Journal of Inorganic and Organometallic Polymers and Materials*, *21(3)*, 602-610. http:/doi.org/10.1007/s10904-011-9494-6

[28] Kürkçüoğlu, G. S., Sayin, E. & Şahin, O. (2015). Cyanide bridged hetero-metallic polymeric complexes: Syntheses, vibrational spectra, thermal analyses and crystal structures of complexes $[M(1,2\text{-dmi})_2\ Ni(\mu\text{-}CN)_4]_n$ (M = Zn (II) and Cd (II)). *Journal of Molecular Structure*, *1101*, 82-90. https://doi.org/10.1016/j.molstruc.2015.08.013

[29] Kürkçüoğlu, G. S., Hökelek, T., Yesilel, O. Z. & Aksay, S. (2008). Synthesis, IR spectrum, thermal property and crystal structure of cyano-bridged heteronuclear polymeric complex, [Cd(teta)Ni(mu-CN)(2)(CN)(2)] center dot 2H(2)O. *Structural Chemistry*, *19(3)*, 493-499. http:/doi.org/ 10.1007/s11224-008-9309-8

[30] Paharova, J., Cernak, J., Zak, Z. & Marek, J. (2007). Use of multi-N-donor ligands for preparation of organic–inorganic hybrid materials: Crystal structures of ionic $[M(aepn)_2][Ni(CN)_4]\cdot H_2O$ and polymeric $M(aepn)Ni(CN)_4$ (M=Zn(II), Cd(II); aepn=N-(2-aminoethyl)-1,3-propanediamine). *Journal of Molecular Structure*, *842*, 117-124. http:/doi.org/10.1016/j.molstruc.2006.12.022

[31] Collins, J. B., Schleyer, P. v. R., Binkley, J. S. & Pople, J. A. (1976) Self-Consistent molecular orbital methods. 17. Geometries and binding energies of second-row molecules. A comparison of three basis sets. *Journal of Chemical Physics*, *64*, 5142-5151. http:/doi.org/10.1063/1.432189

[32] Frisch, M. J., Trucks, G. W., Schlegel, H. B., Scuseria, G. E., Robb, M. A., Cheeseman, J. R., Montgomery, Jr. J. A., Vreven, T., Kudin, K. N., Burant, J. C., Millam, J. M., Iyengar, S. S., Tomasi, J., Barone, V., Mennucci, B., Cossi, M., Scalmani, G., Rega, N., Petersson, G. A., Nakatsuji, H., Hada, M., Ehara, M., Toyota, K., Fukuda, R., Hasegawa, J., Ishida, M., Nakajima, T., Honda, Y., Kitao, O., Nakai, H., Klene, M., Li, X., Knox, J. E., Hratchian, H. P., Cross, J. B., Bakken, V., Adamo, C., Jaramillo, J., Gomperts, R., Stratmann, R. E., Yazyev, O., Austin, A. J., Cammi, R., Pomelli, C., Ochterski, J. W., Ayala, P. Y., Morokuma, K., Voth, G. A., Salvador, P., Dannenberg, J. J., Zakrzewski, V. G., Dapprich, S., Daniels, A. D., Strain, M. C., Farkas, O., Malick, D. K., Rabuck, A. D., Raghavachari, K., Foresman, J. B., Ortiz, J. V., Cui, Q., Baboul, A. G., Clifford, S., Cioslowski, J., Stefanov, B. B., Liu, G., Liashenko, A., Piskorz, P., Komaromi, I., Martin, R. L., Fox, D. J., Keith, T., Al-Laham, M. A., Peng, C. Y., Nanayakkara, A., Challacombe, M., Gill, P. M. W., Johnson, B., Chen, W., Wong, M. W., Gonzalez, C. & Pople, J. A. (2004). Gaussian 03 Revision D.01. Gaussian, Inc., Wallingford CT.

[33] Dennington, R., Keith, T. & Millam, J. (2007). Gauss View, Version 4.1.2. Semichem Inc., Shawnee Mission.

[34] Becke, A. D. (1993). Density-functional thermochemistry. III. The role of exact exchange. *Journal of Chemical Physics*, *98*, 5648–5652. http:/doi.org/10.1063/1.464913

[35] Lee, C., Yang, W. & Parr, R. G. (1988). Development of the Colle-Salvetti correlation-energy formula into a functional of the electron density. *Physical Review B*, *37*, 785–789. http:/doi.org/ 10.1103/PhysRevB.37.785

[36] Peng, C., Ayala, P. Y., Schlegel, H. B. & Frisch, M. J. (1996). Using redundant internal coordinates to optimize equilibrium geometries and transition states. *Journal of Computaional Chemistry*, *17*, 49–56.

[37] Stephens, P. J., Devlin, F. J., Chablowski, C. F. & Frisch, M. J. (1994). Ab Initio calculation of vibrational absorption and circular dichroism spectra using density functional force fields. *Journal of Physical Chemistry*, *98*, 11623–11627. https://doi.org/10.1021/j100096a001

[38] Pearson, P. G. (2005). Chemical hardness and density functional theory. *Journal of Chemical Sciences*, *117*, 5, 369-377. https://doi.org/10.1007/BF02708340

[39] Parr, R. G. & Pearson, R. G. (1983). Absolute hardness: companion parameter to absolute electronegativity. *Journal of American Chemical Society*, *105*, 26, 7512-7516. https://doi.org/10.1021/ja00364a005

[40] Mebi, C. A. (2011). DFT study on structure, electronic properties, and reactivity of cis-isomers of $[(NC_5H_4\text{-}S)_2Fe(CO)_2]$. *Journal of Chemical Sciences*, *123*, 727–731.https://doi.org/10.1007/s12039-011-0131-2

[41] Kumar, C. P. & Buddhadev, M. (2003). HSAB principle applied to the time evolution of chemical reactions. *Journal of American Chemical Society*, *125*, 9, 2705-2710. https://doi.org/10.1021/ja0276063

[42] Nataraj, A., Balachandran, V. & Karthick, T. (2013). Molecular orbital studies (hardness, chemical potential, electrophilicity, and first electron excitation), vibrational investigation and theoretical

NBO analysis of 2-hydroxy-5-bromobenzaldehyde by density functional method. *Journal of Molecular Structure, 1031*, 221–233. http:/doi.org/10.1016/j.molstruc.2012.09.047

[43] Elusta, M. I., Başaran, M. A. & Kandemirli, F. (2019). Theoretical studies on mild steel corrosion inhibition by 5-substituted 1h-tetrazoles in acidic media. *International Journal of Electrochemical Science, 14*, 2743 – 2756. http:/doi.org/10.20964/2019.03.46

[44] Kartal, Z. & Şahin, O. (2022). Synthesis of two Hofmann type and Hofmann-type-like compounds in crystal form from 4-aminopyridine and their characterizations by various methods. *Journal of Molecular Structure, 1252*, 132088. https://doi.org/10.1016/j.molstruc.2021.132088

[45] Spackman, P. R., Turner, M. J., McKinnon, J. J., Wolff, S. K., Grimwood, D. J., Jayatilaka, D. & Spackman, M. A. (2021). CrystalExplorer: a program for Hirshfeld surface analysis, visualization and quantitative analysis of molecular crystals. *Journal of Applied Crystalography, 54(3)*, 1006–1011. http:/doi.org/10.1107/S1600576721002910

[46] Praprotnik, M., Janežič, D. & Mavri, J. (2004). Temperature dependence of water vibrational spectrum: a molecular Dynamics simulation study. *Journal of Physical Chemistry A, 108*, 11056-11062. http://doi.org/10.1021/jp046158d

[47] Carey, D. M. & Korenowski, G. M. (1998). Measurement of the Raman spectrum of liquid water. *Journal of Chemical Physics, 108(7)*, 2669-2675. http://doi.org/10.1063/1.475659

[48] Zhang, C., Khaliullin, R. Z, Bovi, D., Guidoni, L. & Kühne, T. D. (2013). Vibrational signature of water molecules in asymmetric hydrogen bonding environments. *Journal of Physical Chemistry Letters, 4(19)*, 3245-3250. http://doi.org/10.1021/jz401321x

[49] Sharpe, A. G. (1976). *The Chemistry of Cyano Complexes of the Transition Metals*, Academic Press, London.

[50] McCullough, R. L., Jones, L. H. & Crosby, G. A. (1960). An analysis of the vibrational spectrum of the tetracyanonickelate(II) ion in a crystal lattice, *Spectrochimica Acta, 16(8)*, 929–944. https://doi.org/10.1016/0371-1951(60)80057-4